HYDROLOGICAL PROCESSES
Hydrol. Process. **22**, 104–116 (2008)
Published online 27 March 2007 in Wiley InterScience
(www.interscience.wiley.com) DOI: 10.1002/hyp.6687

Subsurface storm flow formation at different hillslopes and implications for the 'old water paradox'

Peter Matthias Kienzler* and Felix Naef
Institute of Environmental Engineering, ETH Zurich, Zurich, Switzerland

Abstract:

Although many studies over the past several decades have documented the importance of subsurface stormflow (SSF) in hillslopes, its formation is still not well understood. Therefore, we studied SSF formation in the vadose soil zone at four different hillslopes during controlled sprinkling experiments and natural rainfall events. Event and pre-event water fractions were determined using artificially traced sprinkling water and ^{222}Rn as natural tracer. SSF formation and the fraction of pre-event water varied substantially at different hillslopes. Both intensity of SSF and fraction of pre-event water depended on whether SSF in preferential flow paths was fed directly from precipitation or was fed indirectly from saturated parts of the soil. Soil water was rapidly mobilized from saturated patches in the soil matrix and was subsequently released into larger pores, where it mixed with event water. Substantial amounts of pre-event water, therefore, were contained in fast flow components like subsurface storm flow and also in overland flow. This finding has consequences for commonly used hydrograph separation methods and might explain part of the 'old water paradox'. Copyright © 2007 John Wiley & Sons, Ltd.

KEY WORDS subsurface storm flow; old water paradox; runoff generation processes; hillslope hydrology; preferential flow; tracer techniques; radon-222; sprinkling experiments

Received 16 August 2006; Accepted 22 January 2007

INTRODUCTION

Conceptualizations of storm runoff formation in humid headwater catchments are fundamental to models of contaminant transport and flood prediction. Fast lateral subsurface flow in hillslopes has been observed to contribute substantially to direct runoff (e.g. Hewlett and Hibbert, 1967; Freeze, 1972; Anderson and Burt, 1990; Scherrer, 1997; Jones and Connelly, 2002; Weiler *et al*., 2006). This runoff formation mechanism is, in general, termed 'subsurface storm flow' (SSF). The occurrence and intensity of SSF depends on the existence and geometry of preferential flow paths and is affected by soil type, biological activity, soil water content and precipitation characteristics (Scherrer and Naef, 2003). However, how these factors act together in the formation of SSF is not yet well understood.

This limited understanding of SSF formation is highlighted by the ongoing event/pre-event water debate. According to results of natural tracer studies (e.g. Fritz *et al*., 1976; Sklash and Farvolden, 1979; Pearce *et al*., 1986), a high percentage of storm flow consists of 'pre-event water' or 'old water' that was present in the catchment before the precipitation event. This finding, however, contradicts common simple concepts of runoff generation (Kirchner, 2003). In quickly responding rivers, mainly surface flow processes are thought to contribute to runoff. Thus, this runoff should contain only little pre-event water. Processes with high fractions of pre-event water, like groundwater flow, are usually considered too slow to produce rapid discharge responses.

Various theories try to explain the high fractions of pre-event water in quickly responding rivers (Buttle, 1994). For example, Sklash and Farvolden (1979) concluded that groundwater contributes substantially to storm runoff by the 'capillary fringe effect' or 'groundwater ridging' in riparian zones. This mechanism has since been discussed controversially. McDonnell and Buttle (1998) and Cloke *et al*. (2006) conclude that the 'capillary fringe groundwater ridging hypothesis' can explain high proportions of pre-event water only in a limited number of riparian zone settings. Other recent studies emphasized the critical role of soil water chemistry, residence time and hydrodynamic mixing processes within the riparian zone (Bishop *et al*., 2004; Burt, 2005; Jones *et al*., 2006).

Fewer studies have dealt with processes on hillslopes. McDonnell (1990) postulated pre-event water discharge through preferential flow in the Maimai catchment (New Zealand). He proposed that event water might infiltrate quickly through macropores into the subsoil, where it backs up into the subsoil matrix and forms a saturated layer above the bedrock. Thus, a small amount of event water mixes with large amounts of pre-event water stored in the subsoil matrix. This mixture drains rapidly downslope through lateral soil pipes at the soil–bedrock interface. In contrast, Torres *et al*. (1998) and Williams *et al*. (2002) proposed pressure propagation effects that lead to the displacement of pre-event water on hillslopes. Referring to this equivocal discussion, McGlynn *et al*. (2002) stated that 'the roles of pressure wave propagation

* Correspondence to: Peter Matthias Kienzler, Institute of Environmental Engineering, ETH Zurich, Schafmattstrasse 6, 8093 Zurich, Switzerland. E-mail: kienzler@ifu.baug.ethz.ch

and particle velocity for the rapid effusion of old water are not yet understood'.

Thus, the objectives of this study are to develop a better understanding of SSF formation on hillslopes and to elucidate how rapid pre-event water contributions to stormflow might originate from SSF. Controlled experiments were replicated across four different slope types ('Test slopes' section) to observe SSF characteristics with hydrometric measurements and tracer injections during sprinkling experiments and natural rainfall events. Additionally, pre-event water was identified in different flow components by using artificially traced sprinkling water and the natural tracer ^{222}Rn ('Methods' section). Different forms of SSF with widely varying pre-event water fractions were observed at the four sites ('Subsurface stormflow formation at different hillslopes' section). Both SSF intensity and fraction of pre-event water depended on whether SSF originated directly from precipitation or indirectly from saturated parts of the soil. The experiments showed that fast-responding, near-surface SSF can already deliver substantial amounts of pre-event water to the stream ('Discussion' and 'Conclusions' sections).

TEST SLOPES

As every hillslope is unique, with a different soil type, depth, and geometry of preferential flow paths, McDonnell (2003) proposed intercomparison of different sites to extract commonalities of runoff response and the influence of local soil and geology parameters. Work has been done in this respect by Scherrer (1997) and Uchida *et al.* (2005, 2006). Following this idea, we observed SSF formation on four test slopes with different soils and geology to cover a range of different subsurface flow paths. At all sites, substantial SSF was expected according to the decision scheme of Scherrer and Naef (2003).

The four test sites, listed in Table I, were situated in the Swiss Plateau. Mean annual temperature in this area is between 6 and 8 °C, mean annual precipitation ranges from 1000 to 1500 mm, and evapotranspiration is about 40% of annual precipitation. The Swiss Plateau is mainly formed by 'molasse', deposited at the border of the Alps and consisting of sandstones, marl, and conglomerates. These sedimentary rocks are in large parts overlain by glacial till and fluvial deposits. Details on geology and soil at the test sites are given in the 'Subsurface stormflow formation at different hillslopes' section and Table II. Land use and vegetation are similar at the four test sites. All four sites are extensively used as meadow. Accordingly, vegetation consists of plants typical for rich pastures, like *Ranunculus acris* and *Dactylis glomerata*. An exception in this respect is Koblenz, where the lower part of the hillslope is used agriculturally.

METHODS

Experimental setup and hydrometric measurements

Infiltration and runoff were measured during sprinkling experiments performed with different intensities and during natural rainfall events. Figure 1 depicts the experimental set-up. The device for high sprinkling intensities of 40–50 mm h^{-1} has already been used by Scherrer (1997) and Faeh (1997). Uniform sprinkling over an area of 110 m^2 was achieved with 15 sprinklers arranged in three lines. For lower intensities of about 10 mm h^{-1}, two garden sprinklers were used. Sprinkling intensity and uniformity of sprinkling were determined with seven small rain gauges. A tipping-bucket gauge recorded natural precipitation.

We measured SSF above the bedrock in an 8 m long trench at the lower end of the hillslope. Surface runoff and outflow from larger pipes and macropores were also measured either with 100 ml tipping-bucket gauges or with 45° Thompson weirs.

Twelve tensiometers recorded the matric potential every 5 min at four different depths. They were arranged in three nests 2 m, 4 m and 6 m upslope of the trench face (Figure 1). The instruments were covered with white-coloured plastic foil to reduce radiative heating. An antifreeze compound was used in winter.

Water content changes in the soil were monitored 2 m and 6 m upslope the trench face with five-segment time-domain reflectometry (TDR) probes, which recorded the average moisture content in 5 min intervals at 0–15, 15–30, 30–45, 45–60 and 60–90 cm depths (Figure 1). TDR probes were applied to get an estimate of where and how much water was stored within the soil profile. The information was used to establish the water balance and to establish a concept of infiltration processes. The probes were calibrated in fine sand substrate. At the Lutertal test slope, 30 TDR waveguides were installed at different depths (Retter *et al.*, 2006).

Six pressure probes recorded the depth to water table every 5 min in piezometers with a diameter of 1″ (25·4 mm). The piezometers were evenly distributed

Table I. Test slope characteristics

Site	Schluessberg	Koblenz	Im Sertel	Lutertal
Location (long., lat.)	8°45′06″, 47°16′48″	8°15′19″, 47°35′30″	7°58′49″, 47°14′17″	8°00′37″, 47°14′10″
Altitude (m a.s.l.)	520	450	540	690
Aspect	SW	NW	NE	S
Slope (%)	28	15	40	30
Slope length (m)	280	330	330	530
Curvature	Concave	Concave	Concave	Concave
Land use	Meadow	Meadow	Meadow	Meadow

DOI: 10.1002/hyp

Table II. Soil characteristics of the test slopes

Site		*Soil classification* Particle size distribution (%)			*Geological parent material*				
Depth (cm)	Horizon	Sand	Silt	Clay	Packing density	Hydraulic permeability (mm h^{-1})	Coarse fragments (%)	Macropore density (m^{-2})	pH
Schluessberg		*Calcaric cambisol*			*Ground moraine*				
0–10	Ah	34	34	32	1.5	19	3	224	5
11–24	A/B	34	34	32	2	19	5	136	5
24–80	Bw	31	35	34	3	8	10	111	5
>80	C	31	35	34	4	3	15	35	8
Koblenz		*Eutric cambisol*			*Loess/moraine*				
0–15	A	26	51	23	1.5	21	<1	162	6
15–45	B	26	53	21	3	8	<1	168	7
45–350	B/C	20	50	30	4	2·5	2–5	214	7
Im Sertel		*Cambisol*			*Sandstone of 'Helvetian' molasse*				
0–20	A	41	29	30	2	24	<1	284	5
20–80	B	47	29	24	2–3	24	<1	216	5
80–160	B/Cv	51	27	22	2–3	24	<1	344	5
160–270	Cv				4	3		126	8
>270	C				5	3			8
Lutertal		*Cambisol*			*Siltstone of 'Oeningian' molasse*				
0–10	A	26	51	23	2	21	<1	184	5
10–25	B	26	51	23	3	8	<1	248	6
25–40	B/Cv	26	51	23	3	8	2–5	132	6
>42	C				5	2·5		0	7

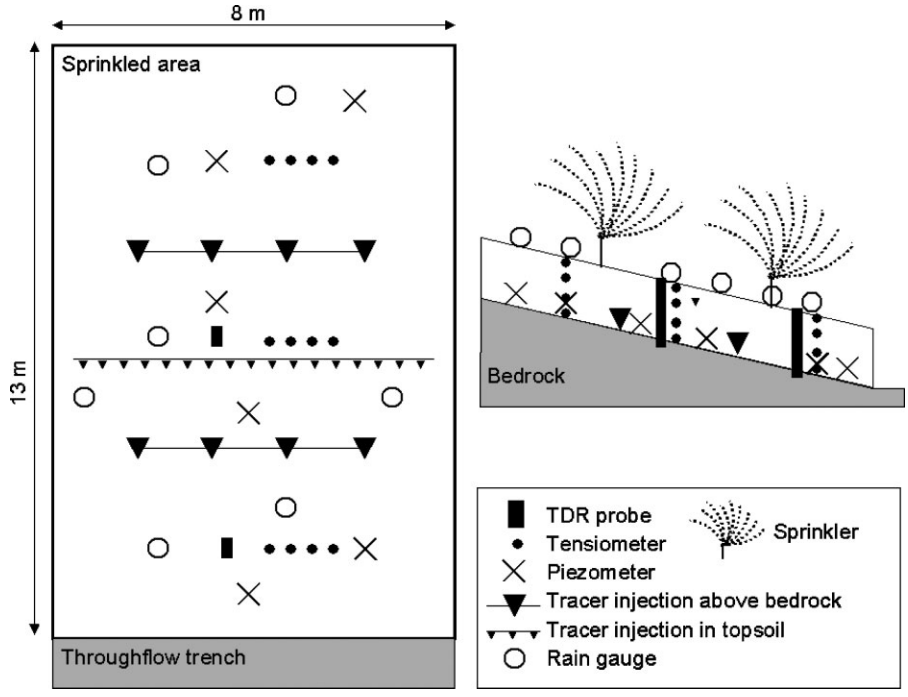

Figure 1. Experimental set-up during the sprinkling experiments in a view from above (left) and in a longitudinal profile (right). Installation depths of the probes and tracer injection varied at different test slopes according to soil depth (Table II)

in the sprinkled area and reached 1·5 to 3 m deep. All tensiometers, piezometers and TDR probes were sealed with clay at the surface to prevent vertical bypass flow along the tubes.

Soil characteristics

Geological and soil characteristics of the test sites are listed in Table II. The particle size distribution was determined with the pipette method. Packing density and percentage of coarse fragments were estimated according to Finnern *et al*. (1994). Values of 'hydraulic permeability' in Table II refer to estimates of saturated hydraulic permeability of the soil matrix after Sponagel *et al*. (2005). They provide a list of hydraulic conductivities with respect to soil type and packing density. Macropore density was assessed by counting the

DOI: 10.1002/hyp

number of macropores in horizontal cross-sections over an area of 2500 cm^2 at different soil depths (every 20 cm). The cross-sections were carefully excavated and cleaned with a brush to avoid destruction or clogging of smaller macropores (radius <1 mm).

Tracer experiments

Artificially traced sprinkling water was used to separate event and pre-event water during the sprinkling experiments. The fluorescent dyes uranine or naphthionate were added to the sprinkling water. Samples of sprinkled water, soil water, outflow from individual macropores and soil pipes, surface and subsurface runoff were taken at least every 15 min. Soil water was collected at 30 and 50 cm depths from six piezometers at three locations. After fluorescence analysis, event-water fraction was calculated from the quotient between outflow concentration and input concentration. Weiler *et al*. (1999), Collins *et al*. (2000) and Buttle and McDonald (2002) have successfully used similar approaches.

To separate event and pre-event water during rainfall events, ^{222}Rn, a decay product of ^{238}U, was used as a natural tracer. Different ^{222}Rn concentrations in groundwater and soil water allow one to quantify contributions of these flow components to stream runoff (Genereux *et al*., 1993). In this study, ^{222}Rn was used to derive the contribution of pre-event water to SSF in the vadose soil zone. There is no ^{222}Rn in the precipitation and, as a noble gas, it does not interact with microorganisms or clay minerals. Water infiltrating into the soil accumulates ^{222}Rn emanating from the soil matrix (DeWayne-Cecil and Green, 1999). The emanation rate is influenced mainly by ^{238}U concentration and by pore volume and pore geometry of the site-specific soil. At the same time, radon is depleted by radioactive decay ($T_{0.5} = 3.8$ days). Thus, the ^{222}Rn concentration reaches a site-specific steady state in soil water or ground water after about 2 weeks (Hoehn *et al*., 1992). Hoehn and von Gunten (1989) used ^{222}Rn to determine ground water residence times of less than 2 weeks.

The device used in our study, a 'Rad 7' instrument from Durridge, measures the radon concentration in air. To bring the dissolved ^{222}Rn into the gaseous phase, a diffusion membrane tube (Accurel) was used. To avoid degassing of ^{222}Rn, the diffusion membrane tube was installed airtight into the outlet of surrounded sources at the hillslope toe (Lutertal, Im Sertel) or directly at the sealed trench (Schluessberg, Koblenz). Thus, we were able to analyse the ^{222}Rn concentration in SSF before the outflow came in contact with air. The use of the ^{218}Po energy window allowed a temporal resolution of about 30 min (Surbeck, 1996). At each test site, the site-specific steady-state ^{222}Rn concentration was determined with permanent measurements over several months and was then used as pre-event water concentration. Thus, pre-event water fraction was calculated from the quotient between outflow concentration and steady-state concentration. Pre-event water fractions determined with radon and with an artificial tracer agreed well (Figure 2), although radon responded more slowly than the artificial tracer. Therefore, ^{222}Rn seems to be well suited to monitor pre-event water fractions in fast subsurface flow in the vadose zone with a high temporal resolution.

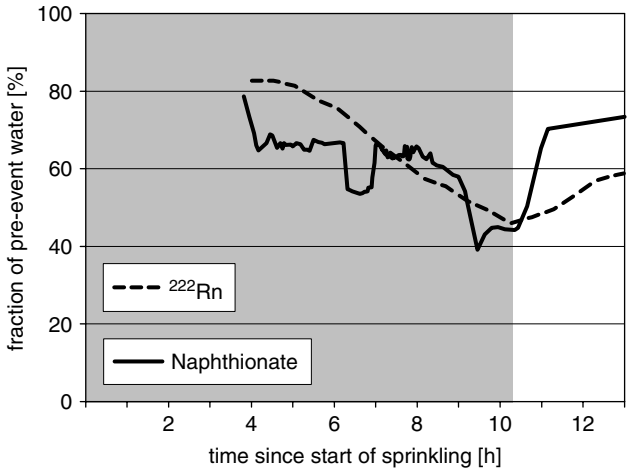

Figure 2. Pre-event water fractions determined with ^{222}Rn and with naphthionate during the low-intensity (11 mm h^{-1}) sprinkling experiment at the Schluessberg test site. The grey shaded area indicates the sprinkling period

To estimate flow velocities, different salt and fluorescent tracers (pyranine, chloride and bromide) were applied instantaneously at different times as line or point sources or over all of the sprinkled area. Three line sources were located at distances of 4, 6 and 8 m parallel to the trench. Tracer was injected at a depth of 15 cm (at the 6 m line) and above the bedrock (at the 4 m line and 8 m line) (Figure 1). Maximum velocities were calculated directly from the tracer breakthrough curve. Recovery rate and mean velocity were estimated by fitting the tracer breakthrough curve to the classical one-dimensional advection–dispersion model.

Measurement errors

Analysis of the salt tracers was made by ion chromatography. A Metrohm 761 device provided an accuracy of 0.2 mg l^{-1} for Br and 0.5 mg l^{-1} for Cl (95% confidence). The accuracy of the fluorescence analysis with a Jobin Yvon Spex Flouromax-2 was 0.3 µg l^{-1} for naphthionate and 0.4 µg l^{-1} for uranine (95% confidence). Uncertainty in the pre-event water fractions was estimated following Genereux (1998). In the sprinkling experiments, pre-event (soil) water did not contain any artificial tracer; during natural rainfall events, event water (precipitation) was clearly defined by the absence of radon. Thus, only uncertainties associated with the artificially traced sprinkling water input, with steady-state radon concentrations and with tracer concentrations in the outflow had to be considered. Uncertainties in pre-event water estimates are given in Table IV.

Conservative behaviour of the tracers naphthionate and uranine is a key assumption for the pre-event water calculations. Therefore, we analysed the sorption strength with soil column experiments with substrates from Lutertal and Im Sertel subsoils. The substrates were

DOI: 10.1002/hyp

dried and sieved (1 mm) and regularly filled into columns of 5 cm diameter and 40 cm height. The columns were carefully wetted and steady-state flow maintained during several days before tracer injection. As tracer recovery was $97 \pm 2\%$, tracer sorption could be neglected for the pre-event water calculations.

Uncertainties are also associated with the determination of the water balance at the sites. Although precipitation and outflow were measured directly, soil water storage had to be estimated with TDR measurements. Percolation into the bedrock could only be determined indirectly as the difference between the input and the sum of outflow and soil water change.

SUBSURFACE STORMFLOW FORMATION AT DIFFERENT HILLSLOPES

In this section, detailed site descriptions and results from hydrometric and tracer measurements are presented, together with a description how SSF was formed at each particular site.

Test slope Schluessberg

The Schluessberg slope is situated in the Zuercher Oberland, 30 km east of Zurich, on a typical drumlin formed during the last ice age (Würm). The bedrock at the test site consists of unsorted and compressed ground moraine. Maximum elevation of the Schluessberg is 554 m a.s.l., 50 m above the valley floor. The sprinkled plot, a meadow on the southwest-facing slope, has an inclination of 28%. The soil is a cambisol with a distinct layering and a depth of 70–80 cm at the sprinkled plot. Transition between the soil and the moraine material is smooth and irregular. However, as Table II shows, the packing density and the aggregate stability increase significantly at the moraine surface and the macropore density decreases substantially.

On the Schluessberg test slope, two high-intensity sprinkling experiments (about 40 mm h^{-1}) and one low-intensity sprinkling experiment (11 mm h^{-1}) were performed. Radon concentrations in the subsurface flow and hydrometric parameters were observed continuously between June 2003 and December 2004.

Here, results are presented of the high intensity sprinkling experiment of 20 June 2003, when 164 mm were sprinkled with an average intensity of 37 mm h^{-1}. Overland flow and outflow from six individual macropores started simultaneously after 45 min (Figure 3). The active macropores were situated 15–40 cm below the surface in the middle part of the trench face. Macropore flow reached a maximum of 7 mm h^{-1} and overland flow a maximum of 25 mm h^{-1}. The cumulative runoff coefficient reached 50%. Soil moisture in the uppermost 15 cm of the soil increased rapidly and strongly, whereas the subsoil moisture content also responded rapidly, but only weakly to the sprinkling. Soil suction measurements showed a quick saturation of the topsoil, whereas the subsoil remained unsaturated. After the sprinkling had been stopped, both overland flow and macropore flow ceased within minutes.

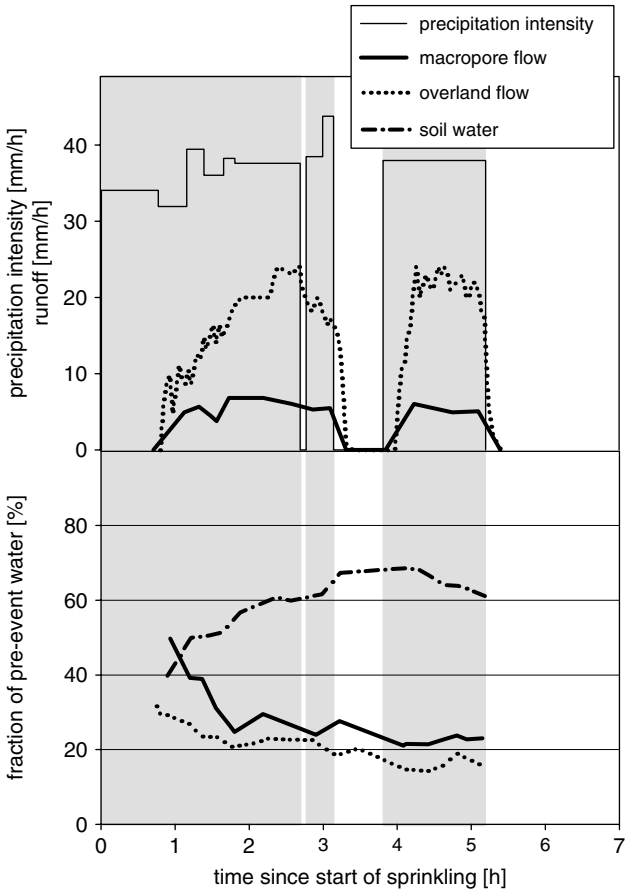

Figure 3. Precipitation intensity, runoff and fraction of pre-event water during the sprinkling experiment at Schluessberg on 20 June 2003. The grey shaded areas indicate sprinkling periods

Figure 3 also shows pre-event water fractions during this experiment. Overland flow started with 30% pre-event water, which decreased to 14%. Macropore flow consisted of 50% pre-event water, dropping to 24% within 1 h. Soil water samples started with concentrations of 40% pre-event water, which increased to 70%.

Despite the high macroporosity, infiltration into the subsoil was limited. Therefore, the uppermost 15 cm of the soil saturated nearly independently from subsoil water content. This topsoil saturation triggered overland flow and flow from individual macropores. Such perched saturation has been observed repeatedly in podzolic soils with a thick organic O-horizon overlaying a distinctive impermeable hardpan layer (Chapell *et al*., 1990; McDonnell *et al*., 1991; Jenkins *et al*., 1994; Brown *et al*., 1999). In our experiments, however, the development of a perched saturation during high-intensity rainfall was caused by slight vertical contrasts of macroporosity and packing density. The comparable fractions of pre-event water in the overland flow and in the macropore flow indicate an intense exchange between overland flow and shallow subsurface flow in the uppermost 10–15 cm of the soil through return flow and reinfiltration.

DOI: 10.1002/hyp

Infiltration into the subsoil was not completely inhibited. The rapid change of subsoil moisture content gives evidence of preferential infiltration into the subsoil of about 14 mm h^{-1}, estimated on the basis of hydrometric measurements. Therefore, in a follow-up experiment with 11 mm h^{-1}, all the water infiltrated into the subsoil. Measurements of soil moisture and soil suction showed no saturation of the uppermost thin soil layer and no overland flow occurred. Instead, subsoil saturation and subsequent SSF from the subsoil occurred due to a reduction of the hydraulic conductivity between the soil and the underlying ground moraine material (Tables III and IV).

Test slope Koblenz

The site is located on a north-facing slope in the small Steingraben catchment (4·8 km^2), which drains directly into the River Rhine. The upper part of the site is used as meadow and the lower part for corn production. The soil has high silt content and a depth of more than 3·5 m (Table II). The geological underground consists of loess, underlain by Würm conglomerates and impermeable Jurassic Opalinus clay.

Despite the low hydraulic conductivity of the deep soil, fast subsurface flow occurred over 115 m on the Koblenz test slope (Weiler and Naef, 2003). Subsurface flow, overland flow and radon concentrations in the subsurface flow were measured at the hillslope toe during natural rainfall events between May 2004 and April 2005. Additionally, water levels and soil suction were recorded in piezometers and tensiometers 40 m and 115 m upslope the flow collector.

Here, results are presented from the largest rainfall event of this period, on 3 June 2004 (Figure 4). Rainfall sum was 57 mm within 24 h. In response, overland flow reached 0·6 mm h^{-1} and subsurface flow increased to 1·1 mm h^{-1}. During this event, 2·6 kg sodium bromide were injected instantaneously in four piezometers 115 m upslope of the flow collector. The tracer arrived 63 min later at the outlet (Figure 4). Thus, the maximum velocity was 3 cm s^{-1}. The average velocity was 0·6 cm s^{-1}. In an experiment during dry conditions with uranine as tracer, the maximal velocity was 1·8 cm s^{-1} and the average velocity was 0·2 cm s^{-1}. Tracer recovery rate was 6·7% during the rainfall event and 0·03% during dry weather conditions. The radon measurements during the event showed a rapid decline of pre-event water in subsurface flow to less than 20% (Figure 4).

Such high subsurface velocities are only possible in long and well-connected flow paths. In fact, outflow has been observed from several large soil pipes with diameters of more than 0·2 m during rainfall events. Concentrated flow was also located with ground-penetrating radar, when highly concentrated sodium chloride solution was injected as a line source into the soil to enhance the radar reflections. After the tracer injection, several point radar reflections were visible at a depth between 1·5 and 2·5 m, indicating shallow lateral soil pipes (Kienzler and Naef, 2006). In the soil matrix with a

Table III. Water balance during the different sprinkling experiments and natural rainfall events. In addition to the experiments explained in detail (italics), follow-up experiments with different sprinkling intensities are listed. Soil water storage is here related to that point in time when SSF ceased

	Schluessberg			Koblenz	Im Sertel		Lutertal	
Date	13/1/04	10/6/04	*20/6/03*	*3/6/04*	*5/8/04*	11/8/04	*3/11/04*	27/5/05
Precipitation intensity (mm h^{-1})	3·1	11·0	37·2	2·4	8·5	51·4	11·6	50·4
Precipitation sum (mm)	117	126	*164*	*57*	*163*	118	*152*	194
Total flow (mm)	35	43	*84*	*10*	*21*	33	*58*	72
Subsurface flow (mm)	35	42	*No SSF*	*9*	*21*	6	*53*	20
Overland flow (OF) (mm)	No OF	1	64 + 20	*1*	*No OF*	27	*5*	52
Soil water storage (mm)	26	33	*27*	*24*	*74*	56	*33*	66
Percolation into bedrock	56	50	*53*	*23*	*75*	30	*62*	60

Table IV. Pre-event water quantities during the different sprinkling experiments and natural rainfall events. In addition to the experiments explained in detail (italics), follow-up experiments made with different sprinkling intensities are listed. At Schluessberg, the runoff generation mechanism changed with increasing precipitation intensity (see 'Test slope Schluessberg' section). Thus, different parts of the soil profile were considered to estimate total amount of pre-event soil water. Error bars on the pre-event water fractions ($x \pm y$) were determined after Genereux (1998)

	Schluessberg			Koblenz	Im Sertel		Lutertal	
Date	13/1/04	10/6/04	*20/6/03*	*3/6/04*	*5/8/04*	11/8/04	*3/11/04*	27/5/05
Event water input (mm)	117	126	*164*	*57*	*163*	118	*152*	194
Pre-event soil water (mm)	180[a]	250[a]	*45*[b]	*1200*	*540*	620	*130*	170
Pre-event water outflow (mm)	23	27	*20*	1·5	*21*	7·5	*32*	16
Pre-event water fraction in SSF (%)	66 ± 6	62 ± 3	*No SSF*	17 ± 9	98 ± 1	95 ± 5	57 ± 8	45 ± 6
Pre-event water fraction in overland flow (OF) (%)	No OF	24 ± 7	24/27 ± 12[c]	?	*No OF*	7 ± 6	26 ± 12	13 ± 8

[a] Whole soil profile of 80 cm.
[b] Only uppermost soil layer of 15 cm.
[c] Overland flow/macropore flow.

DOI: 10.1002/hyp

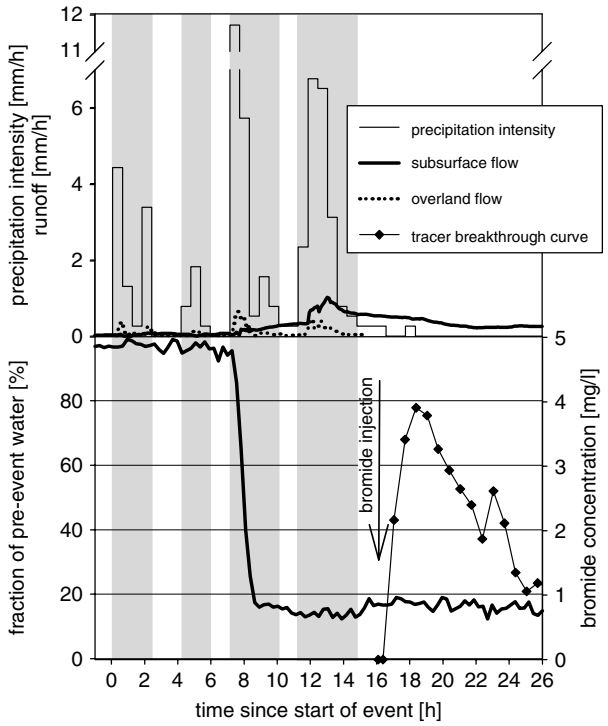

Figure 4. Precipitation intensity, runoff and fraction of pre-event water during a rainfall event at Koblenz on 3 June 2004. The grey shaded areas indicate precipitation periods. Towards the end of the rainfall event, sodium bromide was injected 115 m upslope of the flow collector

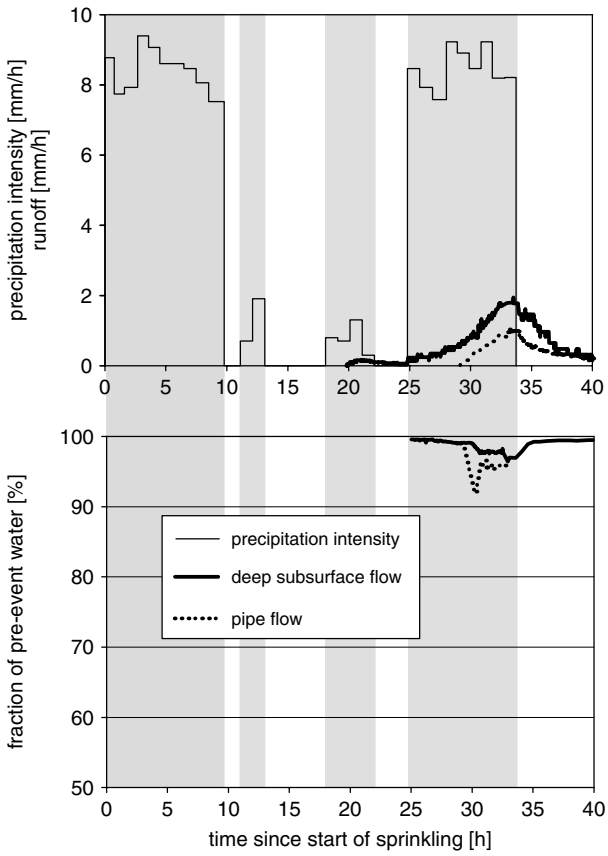

Figure 5. Precipitation intensity, runoff and fraction of pre-event water during the sprinkling experiment at Im Sertel on 5–6 August 2004. The grey shaded areas indicate sprinkling periods

low hydraulic conductivity, thin sandy layers exist. These layers might be starting points for the development of lateral soil pipes through subterranean erosion. Botschek *et al*. (2002) observed such soil pipes in similar soils. As subsurface flow responded quickly to rainfall and consisted mainly of event water, it had to be fed directly by precipitation with a low interaction with the soil matrix. At this site, Weiler (2001) also observed low interaction between vertical macropore flow and the surrounding soil matrix.

Test site Im Sertel

At the test site Im Sertel the soil has a depth of 1·6 m underlain by dense molasse sandstone of the Helvetian period. Estimates based on grain size distribution and packing density revealed a high hydraulic permeability of the soil matrix at Im Sertel. A thin layer of weathered sandstone is visible above the bedrock (Table II). The experiments were performed on grassland on a northeast-facing slope with an inclination of 40%.

Here, low-intensity sprinkling (8·5 mm h^{-1}) over two adjacent days and a high-intensity sprinkling experiment (51 mm h^{-1}) were performed in August 2004 (Table III). Radon concentrations and runoff were continuously measured between September 2004 and December 2005. We present results of the 2-day low-intensity sprinkling experiment of 5–6 August 2004.

On the first day, 82 mm were sprinkled in 10 h, producing no runoff at all (Figure 5). Then, 10 h later, natural rainfall of 5·7 mm triggered a small amount of 'deep SSF' in the thin, weathered layer directly above the sandstone bedrock. When another 75 mm was sprinkled with 8·5 mm h^{-1} on 6 August, SSF increased to 2 mm h^{-1}. At 4·5 h after the start of this second sprinkling period, flow out of a soil pipe in 0·7 m depth started and reached 1 mm h^{-1}. Both deep subsurface flow and pipe flow continued for 16 h after sprinkling had been stopped. Altogether, 6 mm flowed out of the single pipe. Deep subsurface flow amounted to 12·8 mm. In total, 11·5% of the sprinkled water flowed off as subsurface flow. Overland flow did not occur. According to soil moisture and soil suction measurements, nearly 70% of the sprinkled water was stored in the soil. Some 18·5% percolated into the bedrock. Only the subsoil became saturated. The soil water table rose slowly during the experiment up to 1 m below the surface. Flow velocities of the deep subsurface flow were estimated based on instantaneous tracer injections in two line sources above the bedrock. For the line source 4 m upslope of the trench, an average velocity of 3 cm min^{-1} was found and less than 0·5 cm min^{-1} for the line source 8 m upslope of the trench.

The 'deep subsurface flow' in the thin, weathered layer directly above the bedrock contained 97% pre-event water; the flow from the single pipe had more than 92% pre-event water (Figure 5). During a follow-up high-intensity sprinkling experiment, pipe flow contained 86% pre-event water on average, and deep subsurface flow 95% (Table IV).

DOI: 10.1002/hyp

The response of the site Im Sertel differed from Koblenz. Subsurface flow, although entering the trench in preferential flow paths, consisted of nearly 100% pre-event water and started only after 86 mm of rain. Mean flow velocities were 3 cm min^{-1} in the last 4 m above the trench and 0·5 cm min^{-1} for the last 8 m, compared with 36 cm min^{-1} over 115 m in Koblenz. Short lateral flow paths that are not directly connected to each other are indicated by these relatively low lateral flow velocities and, in particular, by the enormous decrease of lateral flow velocity from the 8 m line source compared with the 4 m line source.

Im Sertel had the highest macropore density of the four sites (Table II), but there was obviously no direct preferential flow to the trench. The tensiometer measurements indicate that the soil profile saturated from below, as macropores transported water preferentially deep into the subsoil. There, substantial infiltration from vertical macropores into the subsoil matrix occurred due to the high hydraulic permeability of the soil matrix. Thus, large amounts of rainfall infiltrated before parts of the subsoil saturated. Then, this saturation initiated lateral preferential flow. This flow consisted mainly of pre-event water, as large amounts of soil water, stored in the pores of the unsaturated soil matrix before the experiment, started to move and feed the lateral preferential flow paths. This mechanism can be called indirect feeding, as SSF was initiated and fed from saturated zones of the soil matrix and not, as in Koblenz, directly from precipitation.

Before the experiment, the 1·5 m deep soil at Im Sertel contained about 540 mm of pre-event soil water. From this large reservoir, merely 21 mm flowed off during the sprinkling experiment (Table IV). This implies that even during the largest storms only a small part of the pre-event water is exchanged with event water.

Test site Lutertal

The small catchment of the 'Luter' river (4·0 km^2) is situated in the Swiss Plateau south of Zofingen (Canton Lucerne). The sprinkled plot has an inclination of 24% and faces southeast. Elevation is 690 m a.s.l., about 200 m above the valley floor (Table I). The bedrock consists of dense molasse siltstone of the 'Oeningian' period. Soil depth varies between 35 and 45 cm. Only subtle changes are observed in this cambisol between the soil horizons, whereas a sharp change of hydraulic conductivity occurs at the interface between soil and bedrock (Table II).

On the Lutertal slope, two low-intensity sprinkling experiments were performed in November 2004 and two experiments with high intensities in May and June 2005 (Table III). Natural rainfall events were observed between November 2004 and January 2006.

During the experiment on 3 November 2004, 152 mm was sprinkled in 13 h with an average intensity of 11·6 mm h^{-1}. SSF started after 2 h out of small lateral pipes with diameters of about 0·5 cm situated directly above the bedrock. With time, additional pipes were activated, some pipes with substantial temporal delay of more than 7 h since start of sprinkling. SSF reached 5 mm h^{-1}; overland flow started after 4 h and did not exceed 0·7 mm h^{-1} (Figure 6).

Soil suction measurements at different depths and different locations showed an irregular distribution of soil saturation. Water levels rose quickly in three wells and then levelled off 20 to 30 cm below the surface just when subsurface flow started. Two other wells responded with more delay and levelled off at greater depths to surface.

The pre-event water fractions in the runoff components are given in Figure 6. In the beginning, pre-event water in the subsurface flow was above 80%, dropping to 50% after 6 h. Immediately after the end of sprinkling, the pre-event water fractions increased. An increase also occurred during a 15 min break made for technical reasons after 11·5 h. Overland flow had a nearly constant pre-event water fraction of about 25%. Pre-event water in the soil decreased from 50% to 40% during the experiment.

SSF consisted mainly of the outflow from eight different pipes. Figure 6 shows the substantial variations of pre-event water amounts emanating from these pipes. The outflow from one pipe remained at over 80% of pre-event water, whereas others dropped quickly to 25%.

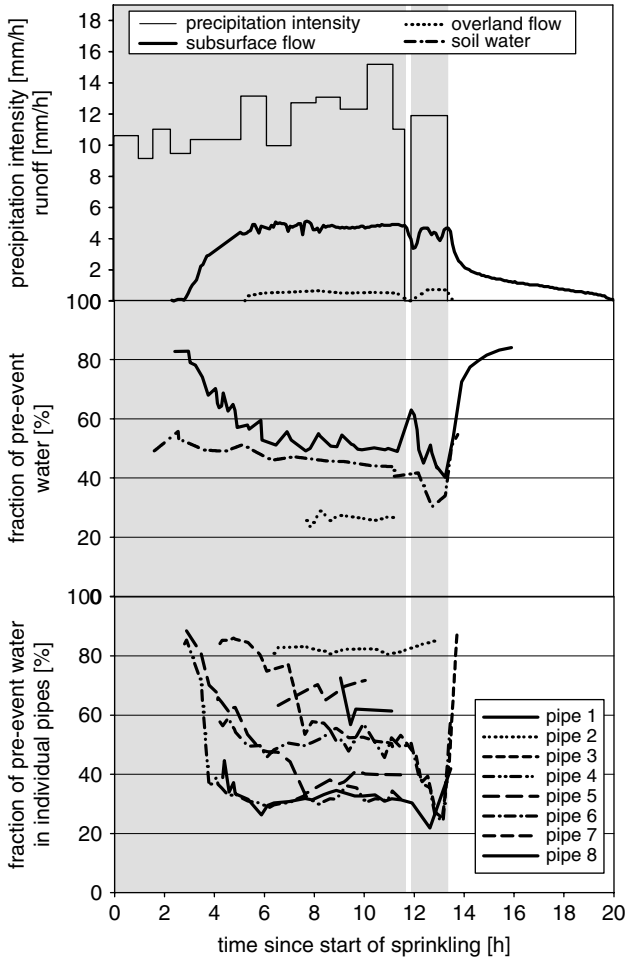

Figure 6. Precipitation, runoff intensity, and fraction of pre-event water during the sprinkling experiment at Lutertal on 3 November 2004. The grey shaded areas indicate sprinkling periods

DOI: 10.1002/hyp

These results were repeated in a follow-up experiment with higher sprinkling intensity.

At Lutertal, the whole soil profile had a high infiltration capability. Water infiltrated quickly due to preferential flow, but substantial infiltration into the soil matrix also happened. The wells and tensiometers showed an irregular moisture distribution, typical for a patchy saturation of the soil. SSF was initiated in lateral pipes when water levels rose above the bedrock surface. Individual lateral pipes started at different times, showing large variation in pre-event water concentrations. Pipes with extended time lags until onset of flow had higher concentrations of pre-event water than pipes starting quickly. In the rapidly responding pipes, SSF was fed directly from precipitation and, therefore, showed a low content of pre-event water. In other parts of the soil the vertical macropores were disconnected from the lateral pipes and flow in these pipes was fed from saturated patches of the soil matrix. Such pipe flow showed an extended time lag and a high fraction of pre-event water, as it was fed indirectly from saturated patches.

Pre-event water concentrations went up quickly after the sprinkling had been stopped. During sprinkling, SSF consisted of event water from directly fed pipes and of pre-event water from indirectly fed pipes. After sprinkling, only the latter continued to contribute to SSF, whereas the direct flow ceased quickly.

DISCUSSION

Direct and indirect feeding of subsurface storm flow

The high-intensity sprinkling experiment at Schluessberg showed that pre-event water can be rapidly mobilized out of saturated parts of the soil profile, even when they are of spatially limited extent. This finding helped us to understand variations of SSF formation and pre-event water percentages at the different test sites. An intercomparison of the sites showed that these variations can be explained with different degrees of direct or indirect feeding of preferential flow: When precipitation feeds directly into preferential flow paths, bypass flow occurs, resulting in a quick SSF response and low pre-event water fractions. In contrast, when preferential flow paths are fed indirectly via saturated parts of the soil, SSF response is delayed and contains much pre-event water.

Koblenz is an example for direct feeding of SSF. Precipitation fed nearly directly an extended system of large and well-connected soil pipes with little interaction with the soil matrix. SSF responded quickly and contained little pre-event water.

In contrast, at Im Sertel, indirect feeding of SSF dominated. Water infiltrated substantially into the soil matrix and subsurface flow was initiated from the saturated subsoil matrix. Therefore, SSF responded only with delay to precipitation and contained little event water.

SSF at Lutertal and Schluessberg responded in between these two extremes. During low-intensity rainfall, parts of the subsoil saturated at Schluessberg and subsequent SSF response was moderately delayed and contained about 60% of pre-event water. At Lutertal, total SSF responded with little delay and contained about 50% of pre-event water. However, flow from individual soil pipes started at different times and contained different amounts of pre-event water. Delayed pipes had higher concentrations of pre-event water than pipes starting quickly. This indicates that the latter were fed directly from precipitation, whereas the former were fed indirectly from saturated parts of the soil. An irregular distribution of saturation in the soil, varying on a small spatial scale, was the reason for this behaviour.

These considerations show that vertical macropores and lateral preferential flow paths might be well connected over considerable distances, being able to transfer event water rapidly and directly into the river. But even if no direct connections exist, efficient water transport is still possible. Vertical macropores can transport water rapidly into the soil, leading to a local saturation of the soil matrix, where pre-event water starts to move and feed lateral preferential flow paths. It is the spatial extent of these saturated zones that determines sensitively the intensity of SSF, as well as the amount of pre-event water in this flow. SSF responds delayed and consists mainly of pre-event water when initiated and fed indirectly from expanded saturation in the soil. However, small, saturated patches within the soil profile may also trigger the onset of lateral preferential flow. This flow responds with little to moderate delay and, accordingly, contains intermediate percentages of pre-event water. In extreme cases, SSF is fed nearly directly from precipitation, and little exchange between the soil matrix and preferential flow takes place. Thus, the variety of SSF formation, which is either fed more indirectly from large saturated zones or fed more directly from small saturated patches, can be referred to as different degrees of direct or indirect feeding of SSF.

Figure 7 and Table V summarize the SSF response and the pre-event water response of the different hillslopes. Tables III and IV give an overview of water balance and pre-event water quantities during the different experiments and natural rainfall events. By comparing the results of the four differently responding hillslopes, the role of direct or indirect feeding of preferential flows became obvious. Directly fed SSF response shows small soil storage until onset of SSF and contains little pre-event water (Koblenz and directly fed pipes at Lutertal). Indirectly fed SSF response is substantially delayed and consists mainly of pre-event water (Im Sertel and indirectly fed pipes at Lutertal). Schluessberg and total SSF at Lutertal respond in between these two extremes.

Implications for the old water paradox

The observations made at Schluessberg showed that pre-event water can even be released from the uppermost thin layer of a soil. During low-intensity rainfall events, when water infiltrates into the subsoil and the uppermost layer is not saturated, pre-event water from this layer is not mobilized and can, therefore, remain there for

DOI: 10.1002/hyp

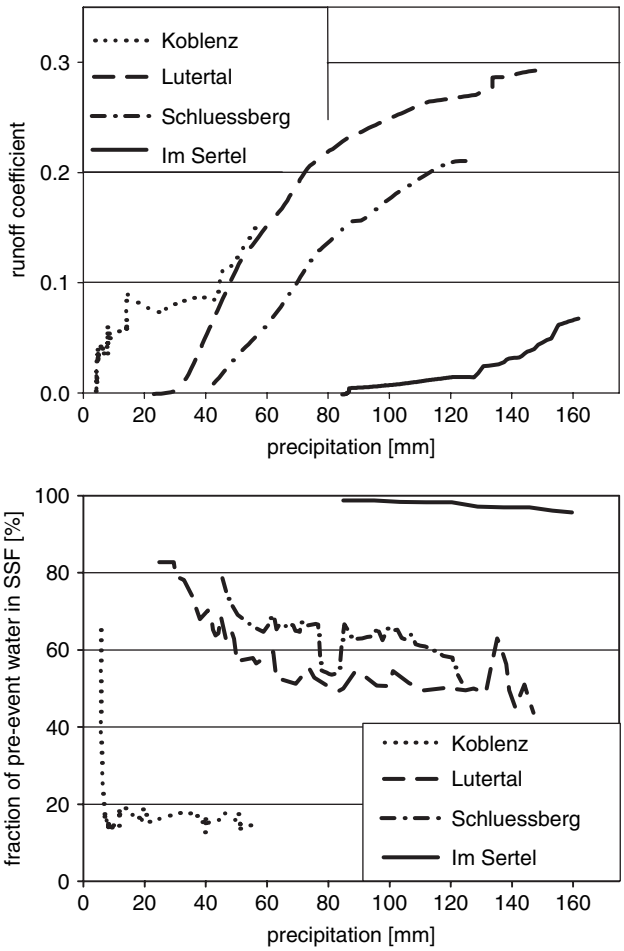

Figure 7. Intercomparison of differently responding hillslopes. Directly fed SSF starts quickly and contains little pre-event water (Koblenz). Indirectly fed SSF starts delayed and consists mainly of pre-event water (Im Sertel)

extended time periods. It can be rapidly mobilized during high-intensity rainfall events, when perched saturation occurs. Usually, hydrograph separation is based on the assumption that overland flow does not contain pre-event water (e.g. Uhlenbrook *et al*., 2002). Pre-event water in overland flow due to an intensive exchange between overland flow and shallow subsurface flow might be quite common and calls this assumption into question.

Similarly, SSF in the uppermost vadose soil zone contained surprisingly high fractions of pre-event water that was released from saturated parts of the soil matrix. Substantial amounts of pre-event water were mobilized even from small, saturated patches irregularly distributed within the soil profile. Obviously, such local saturation of the soil matrix can trigger both, the release of pre-event water and the onset of lateral preferential flow.

These findings imply that even fast flow components from hillslopes, like overland flow and fast subsurface flow, may contain significant amounts of pre-event water. Thus, these flow processes can, at the same time, produce rapid discharge responses and deliver substantial amounts of pre-event water to the stream.

Mixing of rainfall and soil water

Table VI summarizes studies that investigated (in a similar approach to this study) pre-event water fractions in SSF on hillslopes during sprinkling experiments. Large variations of pre-event water content in SSF occurred, which were interpreted differently with regard to processes within the soil profile. For instance, Turton *et al*. (1995) concluded that 'high percentages of old water at the start of each simulation were probably the result of the removal of old water by displacement or diffusion from the inside surfaces of soil macropores'. Buttle and McDonald (2002) found for a forested slope on the Canadian Shield that 'the ability of vertical event water fluxes to participate in lateral subsurface flow was conditioned by the spatial extent of a saturated layer above the bedrock surface'. Anderson *et al*. (1997) pointed out that their 'tracer data calls for a driving mechanism that generates runoff by displacement of

Table V. Direct and indirect feeding of SSF in preferential flow paths

	Koblenz	Lutertal directly fed pipe	Lutertal total SSF	Schluessberg	Lutertal indirectly fed pipe	Im Sertel
	Direct feeding		→		Indirect feeding	
SSF average pre-event water concentration (%)	17	32	57	62	82	98
Soil storage until onset of SSF (mm)	8	24	24	43	77	86

Table VI. Comparison of selected studies that applied artificially traced sprinkling water to assess pre-event water contributions to SSF

Study	Turton *et al*. (1995)	Weiler *et al*. (1999)	Collins *et al*. (2000)	Buttle and McDonald (2002)	Anderson *et al*. (1997)
Event water input (mm)	40–67	195	68	77	275
Average pre-event water fraction in SSF (%)	3·7–31	22·5	44–47	46–62	90–95
Soil storage until onset of SSF (mm)	3–8	20	?	0	0
Sprinkling intensity (mm h^{-1})	13–63	60	2	13	1·6
Area investigated (m^2)	13	60	1137	52	860

DOI: 10.1002/hyp

prestorm water from the vadose zone'. In contrast, Collins *et al.* (2000) observed prolonged outflow of pre-event water and pointed out that this disproves the assumption that pre-event water is displaced as a whole by event water.

In order to obtain insight into the processes responsible for rapid effusion of pre-event water, we analysed how rainfall and soil water, i.e. event and pre-event water, mix in a soil profile and how fast and to what extent pre-event soil water is mobilized. In the following, this topic is discussed on the basis of the Schluessberg high-intensity experiment, where the origin and quantities of pre-event water were clearly defined, as the topsoil responded nearly independently from the subsoil ('Test slope Schluessberg' section). Figure 8 compares the observed pre-event water outflow with a complete and instantaneous mixing between event and pre-event water in the soil as it is usually assumed (e.g. McDonnell, 1990; Weiler and McDonnell, 2004). If a complete mixing is assumed, then the pre-event water fractions pe(t) in the outflow for each time step t_i is

$$\mathrm{pe}(t_i) = \frac{\mathrm{PE}(t_i)}{\mathrm{PE}(t_i) + E(t_i)}$$

where

$$\mathrm{PE}(t_i) = \mathrm{PE}(t_{i-1}) - Q(\Delta \mathrm{t_i})\mathrm{pe}(t_{i-1})$$

and

$$E(t_i) = E(t_{i-1}) + \mathrm{PI}(\Delta t_i) - Q(\Delta t_i)[1 - \mathrm{pe}(t_{i-1})]$$

$\mathrm{PE}(t_i)$ is the amount of pre-event soil water in the uppermost soil layer at time t_i, $E(t_i)$ is the amount of event water in the uppermost soil layer at time t_i, $\mathrm{PI}(\Delta t_i)$ is the precipitation (i.e. event water) input between t_{i-1} and t_i, and $Q(\Delta t_i)$ is the outflow volume between t_{i-1} and t_i (sum of percolation and runoff) is the movable pre-event soil water in the uppermost soil layer at start of flow.

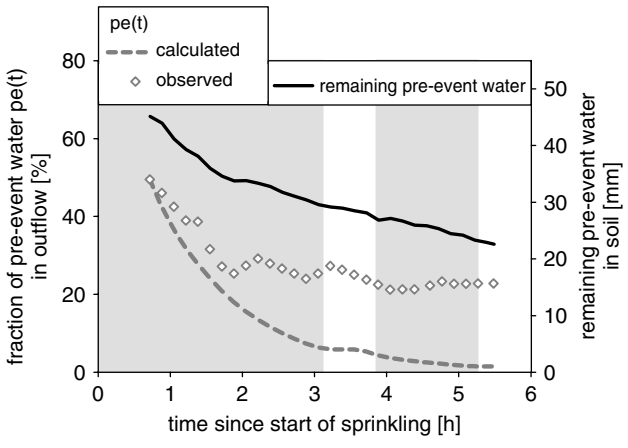

Figure 8. Comparison of observed pre-event water fractions pe(t) and calculated pe(t) assuming a complete mixing and 17 mm of movable pre-event water. The axis on the right-hand side refers to the amount of remaining pre-event water in the uppermost soil layer (solid black line)

The measurements showed that not all potential pre-event water of the topsoil was mobilized when flow started. To match the observed initial fraction of pre-event water, the movable pre-event water has to be reduced. However, in this case the calculated pe(t) cannot predict the prolonged outflow of pre-event water (Figure 8). This disproves clearly the assumption of a complete and instantaneous mixing of event and pre-event water. As the amount of remaining pre-event water in the uppermost soil layer decreased nearly linearly, pre-event water obviously flowed off continuously at a nearly constant rate (Figure 8, solid line, right axis). This may reflect the release of pre-event water only from relatively large pores at the beginning of the experiment. Then, with time, also pre-event water from smaller pores contributed to the flow.

These findings allow no clear answer about whether displacement of pre-event water by pressure waves occurred or not. Further studies have to show theoretically how pre-event water concentrations change over time in the case of pressure wave occurrence (modified by a mixing component). Moreover, there is a need to clarify the spatial scale on which pressure effects may occur. Rasmussen *et al.* (2000) reported observations of pressure waves in laboratory column experiments. Torres *et al.* (1998), as well as Williams *et al.* (2002), postulated the occurrence of pressure waves on the hillslope scale. In our experiment, pressure effects seem to have occurred on the pore scale, when saturation of the soil matrix caused the continuous release of pre-event water into larger pores. There, it mixed with event water and contributed to runoff.

CONCLUSIONS

A combination of hydrometric and tracer measurements and detailed soil investigations made it possible to understand the formation of SSF on four different hillslope test sites. ^{222}Rn was used successfully as a natural tracer to monitor pre-event water fractions in fast subsurface flow with a high temporal resolution.

The formation of SSF and fractions of pre-event water in SSF varied substantially at the four sites. By intercomparison of the different sites, we were able to explain these different responses with different degrees of direct or indirect feeding of SSF. When precipitation feeds directly into preferential flow paths, SSF responds quickly and contains low pre-event water fractions. In contrast, SSF response is delayed and consists mainly of pre-event water when it is fed indirectly via large saturated zones of the soil.

Shallow soil may already contain significant amounts of pre-event water, which can be rapidly released from small, saturated patches of the soil matrix. Such local saturation can also trigger the onset of lateral preferential flow, transporting pre-event water rapidly downslope. Further, the results of this study suggest that an intensive exchange between overland flow and shallow subsurface

DOI: 10.1002/hyp

flow might be quite common. Thus, fast flow components from hillslopes, like overland flow and fast subsurface flow, may, at the same time, produce rapid discharge responses and deliver substantial amounts of pre-event water to the stream. This might explain part of the 'old water paradox'.

ACKNOWLEDGEMENTS

This research was funded by the Swiss Federal Office for the Environment and the European Community Initiative INTERREG III B in the framework of the WaReLa Project. Felix Oberrauch, Saurabh Agarwal, Sebastian Wittmann, Dörte Carstens, Matthias Retter and Dagmar Casper helped with the fieldwork. Wolfgang Kinzelbach, Markus Weiler, Jeff McDonnell and two anonymous reviewers provided invaluable comments to improve this paper. Thank you all very much!

REFERENCES

Anderson MG, Burt TP. 1990. *Process Studies in Hillslope Hydrology*. Wiley.

Anderson SP, Dietrich WA, Montgomery DR, Torres R, Conrad ME, Loague K. 1997. Subsurface flow paths in a steep, unchanneled catchment. *Water Resources Research* **33**: 2637–2653.

Bishop K, Seibert J, Köhler S, Laudon H. 2004. Resolving the double paradox of rapidly mobilized old water with highly variable responses in runoff chemistry. *Hydrological Processes* **18**: 185–189.

Botschek J, Krause S, Abel T, Skowronek A. 2002. Hydrological parameterization of piping in loess-rich soils in the Bergisches Land, Nordrhein–Westfalen, Germany. *Journal of Plant Nutrition and Soil Science* **165**: 506–510.

Brown VA, McDonnell JJ, Burns DA, Kendall C. 1999. The role of event water, a rapid shallow flow component, and catchment size in summer stormflow. *Journal of Hydrology* **217**: 171–190.

Burt TP. 2005. A third paradox in catchment hydrology and biogeochemistry: decoupling in the riparian zone. *Hydrological Processes* **19**: 2087–2089.

Buttle JM. 1994. Isotope hydrograph separations and rapid delivery of pre-event water from drainage basins. *Progress in Physical Geography* **18**: 15–41.

Buttle JM, McDonald DJ. 2002. Coupled vertical and lateral flow on a forested slope. *Water Resources Research* **38**: 1–16.

Chapell NA, Ternan JL, Williams AG, Reynolds B. 1990. Preliminary analysis of water and solute movement beneath a coniferous hillslope in mid-Wales, U.K. *Journal of Hydrology* **116**: 201–216.

Cloke HL, Anderson MG, McDonnell JJ, Renaud JP. 2006. Using numerical modelling to evaluate the capillary fringe groundwater ridging hypothesis of streamflow generation. *Journal of Hydrology* **316**: 141–162.

Collins R, Jenkins A, Harrow M. 2000. The contribution of old and new water to a storm hydrograph determined by tracer addition to a whole catchment. *Hydrological Processes* **14**: 701–711.

DeWayne-Cecil LD, Green JR. 1999. Radon-222 as a tracer in the hydrogeologic environment. In *Isotopes in Subsurface Hydrology*, Cook PG, Herczeg AL (eds.). Kluwer.

Faeh AO. 1997. *Understanding the processes of discharge formation under extreme precipitation. A study based on the numerical simulation of hillslope experiments*. Mitteilungen der VAW, Nr. 150.

Finnern H, Grottenthaler W, Kühn D, Pälchen W, Schraps WG, Sponagel H. 1994. *Bodenkundliche Kartieranleitung*, 4. Auflage. Bundesanstalt für Geowissenschaften und Rohstoffe Bundesrepublik Deutschland: Hannover.

Freeze RA. 1972. The role of subsurface flow in generating surface runoff. *Water Resources Research* **8**: 1272–1283.

Fritz P, Cherry JA, Weyer KU, Sklash MG. 1976. Runoff analysis using environmental isotopes and major ions. In *Interpretation of Environmental Isotope and Hydrochemical Data in Groundwater Hydrology*. IAEA: Vienna; 111–130.

Genereux D. 1998. Quantifying uncertainty in tracer-based hydrograph separations. *Water Resources Research* **34**: 915–919.

Genereux DP, Hemond HF, Mulholland PJ. 1993. Use of ^{222}Rn and calcium as tracers in a three-end-member mixing model for streamflow generation on the West Fork of Walker Branch Watershed. *Journal of Hydrology* **142**: 167–211.

Hewlett JD, Hibbert AR. 1967. Factors affecting the response of small watersheds to precipitation in humid areas. In *International Symposium on Forest Hydrology*, Sopper WE, Lull HW (eds). Pergamon: Oxford; 275–290.

Hoehn E, von Gunten HR. 1989. Radon in groundwater—a tool to assess infiltration from surface waters to aquifers. *Water Resources Research* **25**: 1795–1803.

Hoehn E, von Gunten HR, Stauffer F, Dracos T. 1992. Radon-222 as a groundwater tracer: a laboratory study. *Environmental Science and Technology* **26**: 734–738.

Jenkins A, Ferrier RC, Harriman R, Ogunkoya YO. 1994. A case study in catchment hydrochemistry: conflicting interpretations from hydrological and chemical observations. *Hydrological Processes* **8**: 335–349.

Jones JAA, Connelly LJ. 2002. A semi-distributed simulation model for natural pipeflow. *Journal of Hydrology* **262**: 28–49.

Jones JP, Sudicky EA, Brookfield AE, Park YJ. 2006. An assessment of the tracer-based approach to quantifying groundwater contributions to streamflow. *Water Resources Research* **42**: W02407. DOI: 10·1029/2005WR004130.

Kienzler PM, Naef F. 2006. *How geophysical methods can contribute to subsurface storm flow investigations*. http://www.cosis.net/abstracts/EGU06/03135/EGU06-J-03135.pdf [accessed 5 March 2007].

Kirchner JW. 2003. A double paradox in catchment hydrology and geochemistry. *Hydrological Processes* **17**: 871–874.

McDonnell JJ. 1990. A rationale for old water discharge through macropores in a steep humid catchment. *Water Resources Research* **26**: 2821–2832.

McDonnell JJ. 2003. Where does water go when it rains? Moving beyond the variable source area concept of rainfall–runoff response. *Hydrological Processes* **17**: 1869–1875.

McDonnell JJ, Buttle JM. 1998. Comment on 'A deterministic–empirical model of the effect of the capillary-fringe on near-stream area runoff. 1. Description of the model' by Jayatilaka CJ, Gillham RW. (*Journal of Hydrology*, **184** (1996) 299–315). *Journal of Hydrology* **207**: 280–285.

McDonnell JJ, Owens IF, Stewart MK. 1991. A case study of shallow flow paths in a steep zero-order basin. *Water Resources Bulletin* **27**: 679–685.

McGlynn BL, McDonnell JJ, Brammer DD. 2002. A review of the evolving perceptual model of hillslope flowpaths at the Maimai catchments, New Zealand. *Journal of Hydrology* **257**: 1–26.

Pearce AJ, Stewart MK, Sklash MG. 1986. Storm runoff generation in humid catchments. Where does the water come from? *Water Resources Research* **22**: 1263–1272.

Rasmussen TC, Baldwin RH, Dowd JF, Williams AG. 2000. Tracer vs. pressure wave velocities through unsaturated saprolite. *Soil Science Society of America Journal* **4**: 75–85.

Retter M, Kienzler P, Germann P. 2006. Vectors of subsurface stormflow in a layered hillslope during runoff initiation. *Hydrology and Earth System Sciences* **10**: 309–320.

Scherrer S. 1997. *Abflussbildung bei Starkniederschlägen. Identifikation von Abflussprozessen mittels künstlicher Niederschläge*. Mitteilungen der VAW, Nr. 147, Zürich.

Scherrer S, Naef F. 2003. A decision scheme to identify dominant flow processes at the plot-scale for the evaluation of contributing areas at the catchments-scale. *Hydrological Processes* **17**: 391–401.

Sklash GM, Farvolden RN. 1979. The role of groundwater in storm runoff. *Journal of Hydrology* **43**: 45–65.

Sponagel H, Grottenthaler W, Hartmann KJ, Hartwich R, Janetzko P, Joisten H, Kühn D, Sabel KJ, Traidl R. 2005. *Bodenkundliche Kartieranleitung*, 5. Auflage. Bundesanstalt für Geowissenschaften und Rohstoffe Bundesrepublik Deutschland: Hannover.

Surbeck H. 1996. A radon-in-water monitor based on fast gas transfer membranes. In *International Conference on Technologically Enhanced Natural Radioactivity Caused by Non-Uranium Mining*, Szczyrk, Poland.

Torres R, Dietrich WE, Montgomery DR, Anderson SP, Loague K. 1998. Unsaturated zone processes and the hydrologic response of a steep, unchanneled catchment. *Water Resources Research* **34**: 1865–1879.

Turton DJ, Barnes DR, de Jesus Navar J. 1995. Old and new water in subsurface flow from a forest soil block. *Journal of Environmental Quality* **24**: 139–146.

Uchida T, Tromp-vanMeerveld I, McDonnell JJ. 2005. The role of lateral pipe flow in hillslope runoff response: an intercomparison of non-linear hillslope response. *Journal of Hydrology* **311**: 117–133.

Uchida T, McDonnell JJ, Asano Y. 2006. Functional intercomparison of hillslopes and small catchments by examining water source, flowpath and mean residence time. *Journal of Hydrology*, **327**: 627–642. DOI: 10·1016/j.jhydrol.2006·02·037.

Uhlenbrook S, Frey M, Leibundgut C, Maloszewski P. 2002. Hydrograph separations in a mesoscale mountainous basin at event and seasonal timescales. *Water Resources Research* **38**: 1096. DOI: 10·1029/2001WR000938.

Weiler M. 2001. *Mechanisms controlling macropore flow during infiltration*. Dissertation, ETH Zurich. http://e-collection.ethbib.ethz.ch/show?type=diss&nr=14237 [accessed 5 March 2007].

Weiler M, McDonnell JJ. 2004. Virtual experiments: a new approach for improving process conceptualization in hillslope hydrology. *Journal of Hydrology* **285**: 3–18.

Weiler M, Naef F. 2003. Simulating surface and subsurface initiation of macropore flow. *Journal of Hydrology* **273**: 139–154.

Weiler M, Scherrer S, Naef F, Burlando P. 1999. Hydrograph separation of runoff components based on measuring hydraulic state variables, tracer experiments and weighting methods. In *Integrated Methods in Catchment Hydrology—Tracer, Remote Sensing and New Hydrometric Techniques*, Leibundgut C, McDonnell J, Schultz G (eds). *IAHS Publication* No. 258. IAHS Press: Wallingford; 249–255.

Weiler M, McDonnel JJ, Tromp-van Meerveld I, Uchida T. 2006. Subsurface stormflow. In *Encyclopedia of Hydrological Sciences*, Volume 3, Part 10, Anderson MG, McDonnell JJ (eds). Wiley.

Williams AG, Dowd JF, Meyles EW. 2002. A new interpretation of kinematic stormflow generation. *Hydrological Processes* **16**: 2791–2803.